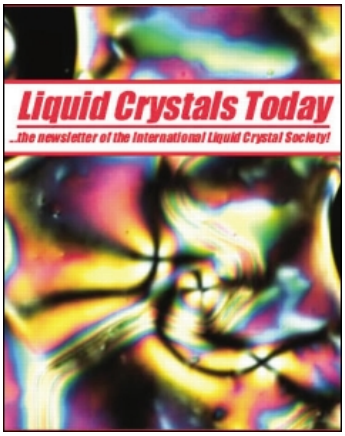

Liquid Crystals Today
Publication details, including instructions for authors and subscription information:
http://www.informaworld.com/smpp/title~content=t713681230

Resonant scattering from liquid crystal devices: an in-situ structural probe for the smectic phases

L. S. Hirst[a]
[a] Liquid Crystal Group, Department of Physics and Astronomy, University of Manchester, UK

Online publication date: 12 May 2010

To cite this Article Hirst, L. S.(2004) 'Resonant scattering from liquid crystal devices: an in-situ structural probe for the smectic phases', Liquid Crystals Today, 13: 3, 15 — 22
To link to this Article: DOI: 10.1080/14645180512331340180
URL: http://dx.doi.org/10.1080/14645180512331340180

LIQUID CRYSTALS TODAY, 2004, VOL. 13, NO. 3, 15–22

Taylor & Francis
Taylor & Francis Group

Resonant scattering from liquid crystal devices: an in-situ structural probe for the smectic phases

L. S. HIRST

Liquid Crystal Group, Department of Physics and Astronomy, University of Manchester, UK

Resonant X-ray scattering is a relatively new technique in the field of liquid crystals and in recent years has been used to investigate the structures of the SmC* sub-phases. This work has been carried out on several materials which include either a sulfur or selenium atom and has revealed the detailed biaxial structure of the four layer intermediate (ferrielectric) phase. Resonant X-ray scattering has also been used to produce the first in-situ measurements of the chiral smectic sub-phases in a liquid crystal device. Both the antiferroelectric and the four-layer intermediate phases have been observed via this technique in a device geometry. Electric field studies have also been carried out in these phases whilst monitoring phase structure simultaneously. In this paper I will summarize the most up-to-date results from resonant scattering in free-standing films and discuss resonant scattering experiments on liquid crystal devices.

Introduction

The chiral smectic liquid crystal phases have been studied in detail since the 1980s as a result of the discovery of several interesting variants to the tilted smectic C phase (SmC), most notably the antiferroelectric phase [1], the ferrielectric, or intermediate phases and the alpha phase [2]. These phases exhibit distinct switching properties which show potential for interesting device applications in optical modulation devices and the display industry.

In the smectic phases, liquid crystal molecules are organized into layers, but within any given layer the molecules have no positional order and are liquid-like. The molecules are oriented along a director (**n**) and this director may be parallel to the layer normal, as in the smectic A phase (SmA) or tilted at an angle to the layer normal as in the smectic C phases (SmC). The differences between the SmC sub-phases can be described by a modulation in the tilt direction on progressing from layer to layer. If the liquid crystal material is also chiral then the director will exhibit an overall helical rotation with a pitch (P_o).

Until relatively recently the structural nature of these chiral SmC* variant phases was somewhat controversial and molecular orientations from layer to layer could only be studied indirectly by electro-optical methods. X-ray scattering is commonly used to directly determine liquid crystal phase structures, however conventional scattering reveals only variations in electron density. This means that the technique is not sensitive to molecular orientations and cannot distinguish between the different SmC* variant phases. Resonant X-ray scattering is a technique which is relatively new to the field of liquid crystals and in recent years has been applied successfully in the study of the smectic C* sub-phases, although resonant or anomalous scattering has been a major technique in protein crystallography for many years.

In our work we have applied resonant scattering to liquid crystal materials. Using an analysis of peak positions and polarization, it is possible to directly probe the interlayer orderings and orientations of the SmC* sub-phases. Conventional X-ray scattering probes variations in electron density in the sample, and peaks are observed at,

$$Q_z = 2\pi l/d = lQ_o \quad (1)$$

Where l is an integer and d is the smectic layer spacing. This means that conventional X-ray scattering will only reveal the layer spacing of a smectic material. However, by scattering at the absorption edge energy of an atom in the liquid crystal molecule, the structure factor for the molecule becomes a tensor and scattering becomes sensitive to molecular orientation. The value of the tensor is dependent on the orientation of the molecule with respect to the polarization direction of the X-ray beam, so extra peaks are observed where there is a periodicity associated with the interlayer tilt orientations and the different phases can be distinguished. The resonant scattering features that have been resolved in

E-mail: linda@mrl.ucsb.edu

Liquid Crystals Today ISSN 1366-5855 online © 2004 Taylor & Francis
http://www.tandf.co.uk/journals
DOI: 10.1080/14645180512331340180

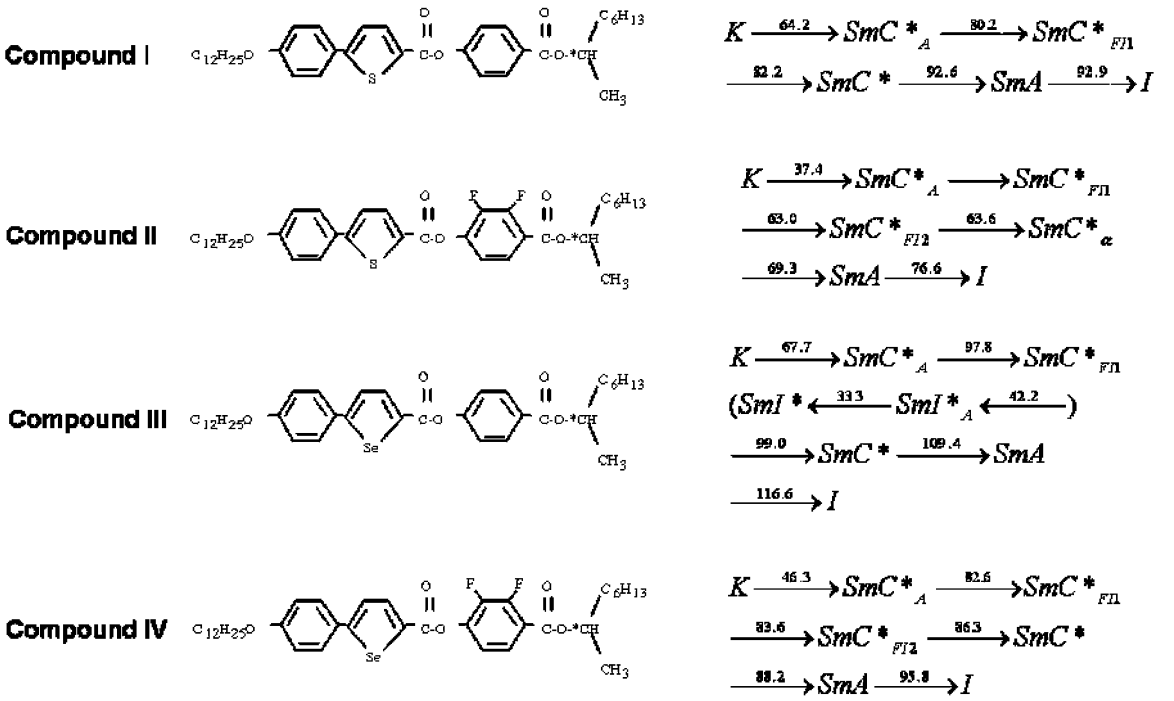

Figure 1. Molecular structures and phase sequences for the liquid crystal materials discussed in this article.

the SmC* sub-phases can be described by assuming a constant interlayer rotation of magnitude

$$2\pi(1/\upsilon+\varepsilon) \tag{2}$$

where υ represents the super-lattice periodicity and ε is the ratio of the smectic layer spacing to the optical pitch. This results in observed resonant scattering peaks at,

$$\frac{Q_z}{Q_o} = l + m(1/\upsilon+\varepsilon) \tag{3}$$

where l and m are integers and $m=0, \pm1$ or ±2.

The polarization of the resonant peaks at $m=\pm1$ and ±2 gives information on the molecular orientations of the liquid crystal molecules from layer to layer, thus it has been exploited as tool to distinguish between the different models for the SmC* phases. The prediction for where resonant peaks should lie and their polarization properties in each of the SmC* phases are described in detail by Levelut and Pansu in their theoretical paper [6].

A synchrotron X-ray source was used in these experiments for its high intensity, polarization properties and potential for energy selection. Resonant features are only detectable at an X-ray energy close to an absorption edge of a specific atom in the material. When scattering is carried out at this absorption edge energy, 'forbidden reflections' from the smectic superlattice can be observed [3]. The liquid crystal materials used in these experiments are special in that they all contain an atom in their rigid core which can be used to provide a resonant X-ray signal, (other resonant scattering studies on materials with the resonant atom on a more flexible part of the molecule (i.e. on the alkyl chains) have been less successful [4]). In this work we used materials designed to contain either sulfur or selenium and the positions of these atoms can be seen in Figure 1 with phase sequences. It should be noted that each material exhibits a rich phase sequence including some or all of the smectic C* sub-phases.

The sulfur and selenium atoms were selected as good candidates based on their K absorption edge, and its accessibility at the synchrotron beam-lines available. Experiments with selenium containing materials were performed on beam-lines 1ID and 1BM at the Advanced Photon Source (APS) at Argonne National Laboratory. For materials containing sulfur, experiments were carried out at the National Synchrotron Light Source at Brookhaven National Laboratory on station X19A. Over the course of this project many different materials containing sulfur, selenium or bromine have been used to observe resonant scattering with varying success. The technique should work well for any atom located in the rigid molecular core with an easily accessible absorption edge energy. All materials shown here were synthesized at the University of Hull

by the Goodby group and exhibit a wide variety of smectic phases at easily accessible temperatures.

Resonant scattering from free-standing films

The first resonant scattering experiments were performed using Bragg diffraction on free-standing smectic films. Thick free-standing films ($\sim$1–5 μm) were prepared for several liquid crystals by drawing material across an aperture [1]. The films were most successfully spread in the SmA phase and could be cooled and reheated into the different SmC* phases using an enclosed oven system. Such films provide an excellent homeotropic alignment and an example of a typical film texture can be seen in Figure 2 for the antiferroelectric phase in compound I.

The films were monitored for defects and thickness by a telescope system mounted to view inside the oven. In this work we aimed for films with a thickness of more than $\sim$500 smectic layers to maximise our scattering intensity. This was estimated by the absence of thin film interference effects. The first work using free-standing films was described by Mach et al. in 1999 [5] who studied sulphur containing materials and observed resonant signals in several of the smectic phases. By polarisation analysis of the peaks at $m = \pm 1$ and ± 2, it was possible to confirm, using the theoretical predictions of Levelut and Pansu [6], that the SmC* phases can be described most accurately by a "clock model" as predicted by several authors [7].

Our more recent free-standing film work, using both sulphur and selenium materials, has helped to complete the picture of the SmC* sub-phase series by observing resonant scattering peaks and their polarisation states in each phase [1, 2]. Figure 3 shows typical resonant

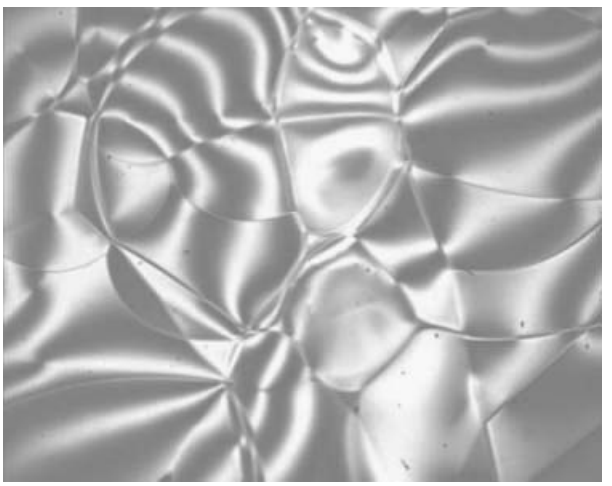

Figure 2. A typical free-standing film texture in the antiferroelectric phase as used for resonant scattering. This image was taken using cross-polarizers in reflection.

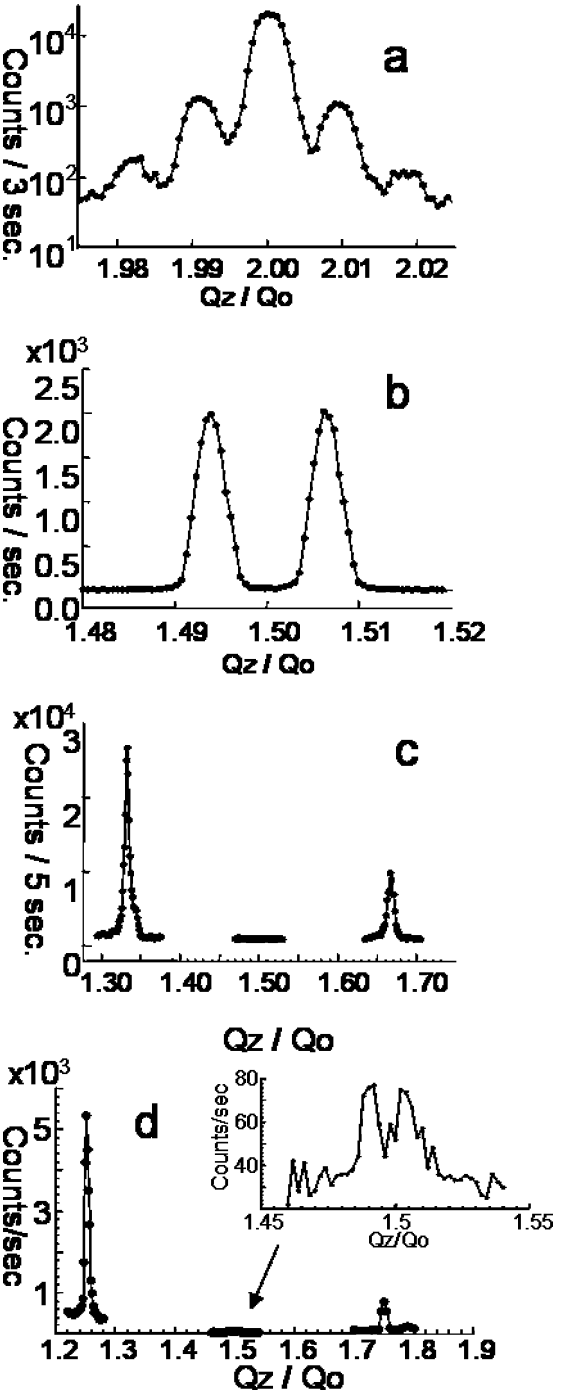

Figure 3. Resonant X-ray peaks in different SmC* subphases, measured at the selenium K edge energy. (a) The ferroelectric phase (SmC*), peaks at $m = -2, -1, 1$ and 2 are shown around the Bragg peak. (b) The antiferroelectric phase (SmC^*_A), peaks at $m = -1$ and 1. (c) The three-layer intermediate phase (SmC^*_{FI1}), peaks at $m = -1$ and 1. (d) The four-layer intermediate phase (SmC^*_{FI2}), peaks at m = −1 and 1 are shown on the main plot and peaks at m = −2 and 2 inset.

Table 1. (Redrawn from ref. 9) A summary of the resonant peaks and their polarization states in each SmC* sub-phase. The table shows which peaks have been observed in free-standing films and those yet to be observed.

Phase	Super-lattice (v)	Peak index (l,m)	Polarization	Peak confirmed	Pol. confirmed
SmC*$_A$	2	1,1	π	√	√
		2,−1	π	√	√
		1,2	σ	√	√
		2,−2	σ	√	√
SmC*$_{FI1}$	3	1,1	π	√	x
		2,−1	π	√	√
		1,2	σ	x	x
		2,−2	σ	x	x
SmC*$_{FI2}$	4	1,1	π	√	√
		2,−1	π	√	√
		1,2	σ	√	√
		2,−2	σ	√	√
SmC*	None	2,−1	σ	√	√
		2,−1	π	√	√
		2,1	π	√	√
		2,2	σ	√	√
SmC*$_\alpha$	Incommensurate	1,1	π	√	√
		2,−1	π	√	x
		1,2	σ	√	x
		2,−1	σ	√	x

scattering data for each of the SmC* phases using selenium as the resonant atom. A summary of the free-standing film results to date is shown in Table I. It should be noted that more work is necessary on the three-layer intermediate phase and the alpha phase to complete the picture.

Biaxiality in the four-layer intermediate phase

One major problem did remain however for the intermediate phase structures after the initial free-standing film work. Although resonant scattering results obtained from films indicated that the four-layer and three-layer intermediate phases were uniaxial, evidence from ellipsometry [10] and conoscopy [11] provided strong evidence that these phases were actually biaxial. This problem suggested that the resonant scattering data was not giving us the whole picture in this phase.

Higher resolution resonant scattering was therefore carried out in the four-layer phase in order to address this problem. It was predicted as an extension to the work of Levelut and Pansu [6], that resonant peaks at $Q_z/Q_0=(0.25-\varepsilon)$, $(0.75+\varepsilon)$...etc. (i.e. m = 1) should be split if the phase is indeed biaxial. Figure 4a demonstrates this biaxiality. The degree of biaxiality of the phase, or δ (the distortion angle) can be calculated from the intensity ratio of the split peaks.

Figure 4b presents the results of higher resolution experiments in the four-layer intermediate phase. Splitting of the resonant peak can clearly be seen at $Q_z/Q_0=(0.75+\varepsilon)$ and similar results were also observed at $Q_z/Q_0=(1.25-\varepsilon)$. This result confirms the prediction that the four-layer intermediate phase is biaxial and a distortion angle (of around 16°) was deduced at different temperatures in the phase [12], a result

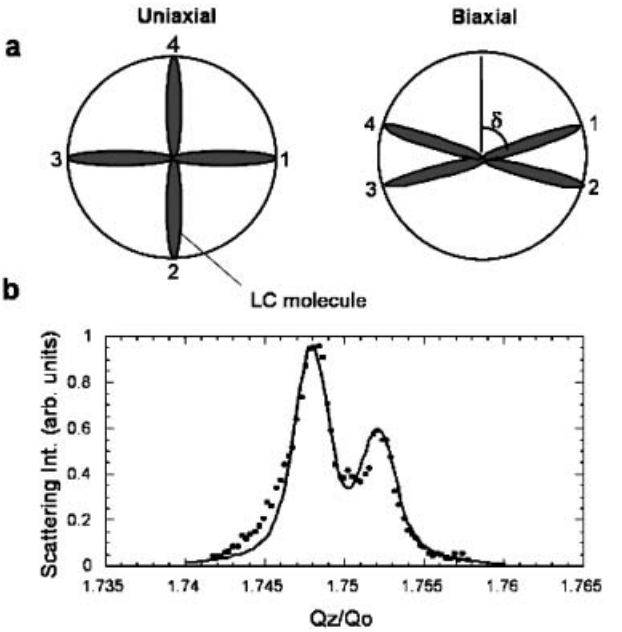

Figure 4. (a) Schematic demonstrating the difference between a uniaxial and a biaxial four layer phase. The numbers indicate the orientational progression from layer to layer and δ is defined as the distortion angle. (b) (redrawn from ref 12) Split resonant scattering data at $m=1$ characteristic of a biaxial structure (points) shown with a predicted peak shape for this structure (line).

consistent with measurements from ellipsometry [13]. Earlier results in this phase did not show the split peaks characteristic of a biaxial structure due to the resolution limits of the experiment. By improving our resolution from 1×10^{-3}Å^{-1} down to 4×10^{-4}Å^{-1} it became possible to reliably resolve this splitting.

The three-layer intermediate phase is also expected to be biaxial, however this is yet to be confirmed. In all the materials discussed in this article the three-layer phase is fairly narrow in temperature range (~1°C) and therefore experimentally it has been difficult work with. Further work on materials with a wider phase window will be necessary to confirm that the three-layer phase is biaxial.

Resonant scattering from liquid crystal devices

For device-based experiments X-ray scattering was carried out in a transmission geometry, therefore consideration was given to minimize attenuation of the X-ray beam. Devices were constructed of 170 μm thick, indium tin oxide (ITO) coated glass. The inner surfaces of the glass plates which formed the device were spin coated with a thin nylon 6/6 alignment layer, which was rubbed on one side with a soft cloth to promote uniform planar alignment of the liquid crystal material. The glass plates were assembled to enclose a 15–30 μm thick liquid crystal sample, defined by a polyethyleneterephthalate spacer. The device was capillary filled with liquid crystal and sealed using an epoxy-resin cement. Figure 5a shows a schematic of the device. The device thickness was chosen to to maximise the X-ray signal whilst also maintaining a good alignment. The ITO glass coating acts an electrode, allowing the application of electric fields across the material, as in a standard LC device. We were able to apply fields up to 5 V/μm.

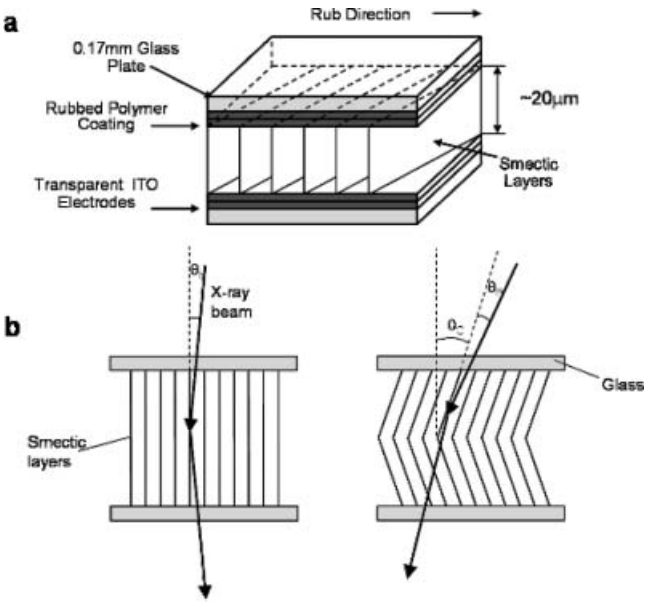

Figure 5. (a) A schematic of the liquid crystal device design and (b) A cartoon demonstrating the bookshelf (left) and chevron (right) layer geometries. The Bragg angle for the smectic layers (θ_B) and the chevron angle (θ_C) are shown.

In order to obtain a good alignment in these thick devices they were filled in the isotropic phase, then slowly cooled into the SmA phase. Heat control was provided by a Linkam [1] hot stage apparatus with a relative accuracy of ±0.05 K. On cooling into the tilted phases the bulk orientation of the smectic layers was taken into account. When a planar device is cooled into the SmA phase the layers will usually lie perpendicular to the glass plates in the "bookshelf" geometry. However on cooling into a tilted smectic phase, such as the SmC* phase these layers buckle to accommodate the layer shrinkage, whilst remaining anchored to the surfaces, normally forming the "chevron" structure [14]. We have taken this into account in our measurements as the device must be first rocked to the chevron angle in the SmC* phases before we can look for scattering from the smectic layers (Figure 5b).

X-rays with an energy at the sulphur absorption edge are strongly absorbed by glass, therefore our experiments concentrated on scattering from selenium containing materials to avoid this problem.

The antiferroelectric phase

The first resonant scattering work on free standing films [5] revealed that distinct peaks characteristic of the antiferroelectric phase can be observed at $Q_z/Q_0=(0.5\pm\varepsilon)$, $(1.5\pm\varepsilon)$ etc. Our initial aim in these device experiments was to observe a resonant signal from inside the device, verifying that the technique would be effective for our system and to allow optimization of the device design [8]. The antiferroelectric phase exhibits the clearest resonant scattering signal in free standing films so this was a good place to start.

Figure 6 shows examples of the resonant scattering signal from the antiferroelectric phase in a device in two different selenium containing materials [15]. The spacing of the two peaks shown for each material is characteristic of the pitch, as determined by equation (3) therefore we are able to measure pitch directly inside a device in the antiferroelectric phase with fairly high accuracy, dependant on the signal to noise ratio of the data. Pitch measurements obtained in this way are consistent with the results from free standing films of the same material. Our device data shown in Figure 6 for material III gives a pitch of 0.55 μm (compared to 0.58 μm in free standing films). The slight difference

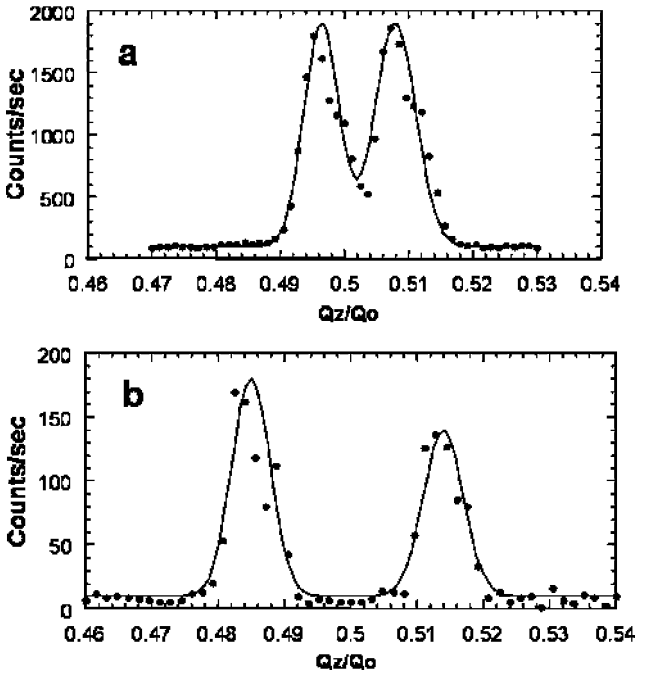

Figure 6. (Redrawn from ref. 15). Resonant peaks in the antiferroelectric phase measured in a liquid crystal device for (a) compound III (85°C) and (b) compound IV 75°C.

between these two measurements is most likely accounted for by a difference in temperature between the film and device heating systems. For compound IV a pitch of 0.24 μm is observed.

The four-layer intermediate phase

Having successfully observed the antiferroelectric phase in devices, we then hoped to observe the intermediate (or ferrielectric) phases exhibited by these materials. Free-standing film work confirmed the phase sequences of compounds III and IV and showed that compound IV forms both the three-layer and the four-layer phases.

Figure 7 shows data in the four layer phase measured in an LC device. This result confirms that the four layer phase is present in the device geometry as well as in free-standing films [15].

To date the three-layer phase is yet to be observed via resonant scattering in an LC device geometry. This may be due to the more delicate nature of this phase (it has also been more difficult to observe in free-standing films) or it may be that in an LC device this phase is suppressed and therefore does not occur. In the materials discussed in this article the three-layer phase is fairly narrow in temperature range ($\sim 1^{\circ}$C) and therefore it has been difficult to work with. Further scattering work on this phase will be performed on materials which exhibit a much wider phase window.

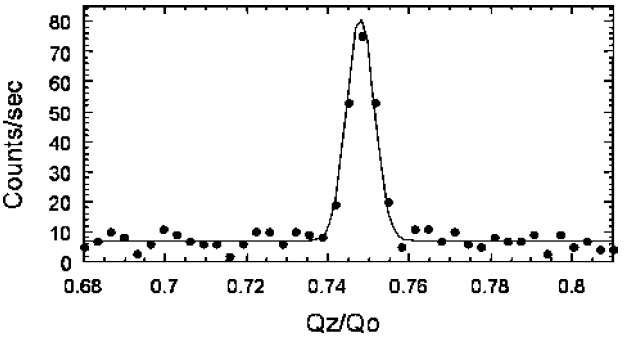

Figure 7. (Redrawn from ref. 15). Resonant peak in the four-layer intermediate phase of compound IV at 86°C measured in a liquid crystal device.

Electric field studies

One of the main advantages to carrying out resonant scattering experiments in a liquid crystal device geometry is that it becomes easy to apply fairly high electric fields across the material parallel to the layer normal. Free standing films are generally spread over a large aperture >5 mm in diameter and as they have a homeotropic alignment it is difficult to achieve high fields. However, in a planar device, of thickness between 10 and 20 μm, we use the standard geometry for ferroelectric switching therefore the application of high fields is routine. Electric fields were applied to the liquid crystal device using a 100 Hz square wave.

In the antiferroelectric phase we investigated two different, well-known phenomena. Helical unwinding at low electric fields has been observed optically in many materials, however optical transmission studies of compound III show no evidence of helical unwinding. In order to confirm that no helical unwinding takes place in this material the positions of the antiferroelectric resonant peaks at $Q_z/Q_0 = 1.5 \pm \varepsilon$ were monitored with increasing electric field strength and the helical pitch calculated. Data acquisition was triggered such that scattering data were only collected during the last 33 ms of the positive part of the field cycle. It was found that as the field was increased stepwise the pitch did remain constant in this material and the resonant peak positions did not change. This result supports the optical measurements which suggest that compound III does not exhibit helical unwinding at low electric fields.

The second phenomenon we looked at was the onset of ferroelectric switching in the device where the antiferroelectric phase structure is forced into a ferroelectric structure by the applied electric field. This occurrence was also monitored via the features at $Q_z/Q_0 = 1.5 \pm \varepsilon$. Fields of successively higher magnitude were applied to the device until the onset of switching, at which point the antiferroelectric peaks disappeared

and the layers in the device also transformed to a bookshelf geometry. This experiment allowed us to confirm that the threshold field for ferroelectric switching in the antiferroelectric phase in compound III is coincident with the chevron to bookshelf transformation.

Devices were also prepared in the four layer intermediate phase for electric field studies using compound IV. Again electric fields of gradually increasing amplitude were applied to the device. The four-layer intermediate phase can show layer re-arrangements at very low fields, i.e. below the onset of switching [16] therefore after each field increment the scattering signal from the Bragg peak at $Q_z/Q_0 = 1$ was optimised for the chevron angle. At an electric field of 0.71 V/μm the device transformed into a bookshelf geometry whilst remaining in the intermediate phase. This phase was still present after the removal of the electric field. Optical transmission studies on this device revealed two distinct transitions with increasing electric field, at 0.7 V/μm and 1.3 V/μm. Using a combination of conventional and resonant scattering we have been able to show that although the device displays some switching behaviour at very low fields the actual transition to ferroelectric switching does not occur until 1.3 V/μm, at a higher electric field than the chevron to bookshelf transformation.

Conclusions

Resonant scattering studies on free-standing films have been extremely successful in elucidating the SmC* variant phase structures. We have clearly observed the resonant features associated with each phase confirming the assumptions of the ''clock model'' for these materials. In addition high resolution resonant scattering has revealed the biaxial structure of the four layer phase and measurements of the distortion angle in this phase have been carried out.

Our group has carried out the first experiments using resonant scattering to probe the smectic inter-layer structures directly in a liquid crystal device. Using materials containing selenium and specially constructed thin devices it is possible to characterise the structure of a phase in-situ whilst simultaneously applying an electric field across the material. We have confirmed the presence of the antiferroelectric phase and the four layer intermediate phase in thick liquid crystal devices in different materials, showing that the resonant scattering data is consistent in this geometry with that measured in free standing films. It will be interesting to investigate if these phases maintain the same structure as we decrease the thickness of the device and to see if the intermediate phases are present in very thin devices.

Pitch measurements have been carried out in these phases and there is clear potential using this technique to look at the pitch in a phase as a function of applied electric field whilst in a device geometry. We have shown in one particular material that there is no evidence of helical unwinding at low electric field, and this conclusion is supported by optical transmission observations. Measurements of the pitch unwinding, until now have been fairly indirect, however using resonant scattering the helical unwinding effects under the application of electric fields can be investigated in many different materials.

We have shown in a previous publication [9] that it is possible to dope a non-resonant material with as little as 10% resonant liquid crystal and still see resonant scattering peaks in the antiferroelectric phase. This dopant percentage can certainly be reduced further, demonstrating a technique with great potential for the study of materials which show interesting electro-optical properties. It may be possible to use a small amount of dopant material to investigate the structure and molecular reorientations of any LC material under different electric field conditions. By triggering the detector at different points in the switching cycle we can investigate phenomena such as bi-stable and tri-stable switching in detail. As the molecules rearrange under the electric field we can capture their orientations and determine different molecular configurations in the field cycle.

Resonant scattering can also be combined with conventional scattering results and other electro-optical measurements as we have shown in this article. It is a powerful technique for structural investigations and may provide important information in the future as part of switching studies. The electric field experiments performed by our group using resonant scattering demonstrate the enormous potential of resonant scattering in this respect, by directly observing molecular configurations under different electric field conditions.

Acknowledgements

Grateful thanks go to the many collaborators I have worked with on this project, most notably to my thesis supervisor, Helen Gleeson and to Ron Pindak. Other collaborators on this project include Phillippe Barois, Anne-Marie Levelut, C.C. Huang and his group (Andy Cady and Patrick Davidson), John Pitney, Samantha Watson and Peter Mach. Additionally I would like to thank John Goodby, Mike Hird and Alex Seed at The University of Hull for the Liquid Crystal materials. I would also like to acknowledge the beam line staff at the National Synchrotron Light Source, at Brookhaven

National Laboratory, and the Advanced Photon Source at Argonne National Laboratory, most notably George Stajer, Jens Pollmann, Wolfgang Caliebe and Lars Furenlid. Without their generous contributions this work would not have been possible. Funding was provided by the EPSRC and Lucent Technologies (CASE award). Additional funding was also provided by the U.S. Dept of Energy Contract no. W-31-109-ENG-38 and by the National Science Foundation, Grant nos. DMR-9703898, DMR-9901739 and INT-9815858.

References

[1] Chandani, A. D. L., Goreka, E., Ouchi, Y., Takezoe, H., and Fukuda, A., 1989, Antiferroelectric chiral smectic phases responsible for the tristable switching in MHPOBC, *Jpn. J. Appl. Phys.*, **28,** L1265.

[2] Fukuda, A., Tananisi, Y., Isozaki, T., Ishikawa, K., and Takezoe, K., 1994, Antiferroelectric chiral smectic liquid-crystals, *J. Mater. Chem.*, **4,** 997.

[3] Dmitrienko, V. E., 1983, Forbidden reflections due to anisotropic X-ray susceptibility of crystals, *Acta. Cryst.*, **A39,** 29.

[4] Cluzeau, P., Gisse, P., Ravaine, V., Levelut, A.-M., Barois, P., Hunag, C. C., Rieutord, F., and Nguyen, H. T., 2000, Resonant X-ray diffraction study of a new brominated chiral SmCA* liquid crystal, *Ferroelectrics*, **244,** 301.

[5] Mach, P., Pindak, R., Levelut, A.-M., Barois, P., Nguyen, H. T., Baltes, H., Hird, M., Toyne, K., Seed, A., Goodby, J., Huang, C. C., and Furenlid, L., 1999, Structures of chiral smectic-C mesophases revealed by polarization-analyzed resonant x-ray scattering, *Phys. Rev. E.*, **60,** 6793.

[6] Levelut, A.-M., and Pansu, B., 1999, Tensorial X-ray structure factor in smectic liquid crystals, *Phys. Rev. E.*, **60,** 6803.

[7] Cepic, M., and Zeks, B., 1995, Influence of competing interlayer interactions on the structure of the Sm C alpha* phase, *Mol. Cryst. Liq. Cryst.,* **263**, 61; Lorman V. L. 1995, Antiferroelectric and ferrielectric structures induced by multilayer ordering in chiral smectics, *Mol. Cryst. Liq. Cryst.*, **262**, 437; Pikin S. A., Hiller S., Haase W., 1995, Short-pitch modes approach to the problem of antiferroelectricity in liquid crystals, *Mol. Cryst. Liq. Cryst.*, **262**, 425; Roy A., Madhusudana N., 1996, A simple model for phase transitions in antiferroelectric liquid crystals, *Europhys. Lett.*, **36**, 221.

[8] Matkin, L. S., Gleeson, H. F., Mach, P., Huang, C. C., Pindak, R., Srajer, G., Pollmann, J., Goodby, J. W., Hird, M., and Seed, A., 2000, Resonant X-ray scattering at the Se edge in liquid crystal free-standing films and devices, *Appl. Phys. Lett.* **76**(14), 1863–1865.

[9] Hirst, L. S., Watson, S. J., Gleeson, H. F., Cluzeau, P., Barois, P., Pindak, R., Mach, P., Pitney, J., Johnson, P., Huang, C. C., Srajer, G., Pollmann, J., Levelut, A.-M., and Caleibe, W., 2002, Interlayer structures of the chiral smectic liquid crystal phases revealed by resonant X-ray scattering, *Phys. Rev. E.* **65**(4), 1705.

[10] Johnson, P. M., Olson, D. A., Pankratz, S., Nguyen, H. T., Goodby, J., Hird, M., and Huang, C. C., 2000, Structure of the liquid-crystal ferrielectric phases as determined by ellipsometry, *Phys. Rev. Lett.*, **84,** 4870.

[11] Baylis, L. J., Gleeson, H. F., Seed, A. J., Styring, P. J., Hird, M., and Goodby, J. W., 1999, Conoscopic observations of multiple ferrielectricity in a chiral liquid crystal, *Mol. Crys. Liq. Crys.*, **328,** 13–20.

[12] Cady, A., Pitney, J. A., Pindak, R., Matkin, L. S., Watson, S. J., Gleeson, H. F., Cluzeau, P., Barois, P., Levelut, A.-M., Caleibe, W., Goodby, J. W., Hird, M., and Huang, C. C., 2001, Orientational ordering in the chiral smectic-C-F12* liquid crystal phase determined by resonant polarized X-ray diffraction, *Phys. Rev. E.*, **64**(5), 702.

[13] Linkam Scientific Instruments Ltd, UK.

[14] Rieker, T. P., Clark, N. A., Smith, G. S., Parmar, D. S., Sirota, E. B., and Safinya, C. R., 1987, Chevron local layer structure in surface-stabilized ferroelectric smectic-C cells, *Phys. Rev. Lett.*, **59,** 2658.

[15] Matkin, L. S., Watson, S. J., Gleeson, H. F., Pindak, R., Pitney, J. A., Barois, P., Levelut, A.-M., Srajer, G., and Pollmann, J., 2001, Resonant X-ray scattering study of the antiferroelectric and ferrielectric phases in liquid crystal devices, *Phys. Rev. E,* **64**(2), 1705.

[16] Watson, S. J., Matkin, L. S., Baylis, L., Bowring, N., and Gleeson, H. F., 2002, Influence of electric fields on the smectic layer structure of ferroelectric and antiferroelectric liquid crystal devices, *Phys. Rev. E.* **65**(3), 1705; Matkin L. S., Gleeson H. F., Baylis L. J., Watson S. J., Bowring N. 2000, Electric field-induced layer deformations in the subphases of an antiferroelectric liquid crystal device, *Appl. Phys. Lett.*, **77**(3), 340–342.